01 Jul 2004

Multilevel Inverters with Equal or Unequal Sources for Dual-Frequency Induction Heating

B. Diong

S. Basireddy

Keith Corzine
Missouri University of Science and Technology

Yakov L. Familiant

Multilevel Inverters With Equal or Unequal Sources For Dual-Frequency Induction Heating

Bill Diong and Sarala Basireddy
Department of Electrical and Computer Engineering
The University of Texas at El Paso
El Paso, TX 79968, USA

Keith Corzine and Yakov Familiant
Department of Electrical Engineering and Computer Science
University of Wisconsin – Milwaukee
Milwaukee, WI 53201, USA

Abstract – Most existing power supplies for induction heating equipment produce voltage at a single (adjustable) frequency. Recently, however, induction heating power supplies that produce voltage at two (adjustable) frequencies have been researched and even commercialized. Dual-frequency power supplies are a significant development for heat-treating workpieces with uneven geometries, such as gears, since different portions of such workpieces are heated dissimilarly at a single frequency and so require a two step process using a single-frequency power supply. On the other hand, a dual-frequency power supply can achieve the desired result for such workpieces in a one step process. This paper proposes the use of multilevel converters for providing induction heating power at two frequencies simultaneously, which may achieve higher efficiency, improved control, reduced electromagnetic interference and greater reliability than existing dual-frequency power supplies. It also describes how the stepping angles for the desired output from such converters can be determined for both the equal and unequal source cases. Furthermore, experimental results are presented as a verification of the analysis.

I. INTRODUCTION

Many industries (automotive, aerospace, biomedical, etc) require the application of heat to targeted workpiece sections as part of processes such as hardening, brazing, bonding (curing), etc. One important environment-friendly approach to such heating is by electromagnetic induction, known as induction heating. Most existing induction heating power supplies produce power at a single (adjustable) frequency. Recently, however, supplies that produce power at two frequencies simultaneously have been investigated [1–4] as well as commercially introduced [5]. This is because for workpieces with uneven geometries, such as gears, different portions of the workpiece are heated dissimilarly at a single frequency and so their processing needs two steps (to allow a frequency adjustment) using a single frequency power supply. Hence, it's extremely desirable to supply dual-frequency power simultaneously to the induction coil to attain the optimal result for such workpieces in just one pass. However, drawbacks of the approach proposed by [1] include the restriction of dual-frequency production to just the 1st and 3rd harmonics and the inability to independently adjust their levels and those of the adjacent (5th, 7th, etc.) harmonics, although some incremental improvements have recently been made to this approach [2–4]. Drawbacks of [5] include the significant power loss caused by the passive components and high-frequency switching part of those units, and the two disparate control methods for the low-frequency and high-frequency sub-circuits.

This paper describes initial studies of a dual-frequency induction heating power supply based on multilevel inverters, which may achieve higher efficiency, reduced electromagnetic interference and greater reliability. Multilevel converters are a recent exciting development in the area of high-power systems. Several topologies exist, including the diode-clamped (neutral-point clamped), capacitor-clamped (flying capacitor), and cascaded H-bridge (Fig. 1), etc. Presently, they are typically operated to produce approximately a single-frequency output voltage (Fig. 2 as example), which could be either fixed (utility) or varying (motor drive) [6]. While [7] has introduced the idea of multilevel inverters for multi-frequency induction heating, few analytical details were provided.

II. ANALYSIS – EQUAL DC SOURCE VALUES

For an output voltage waveform that is quarter-wave symmetric (as in Fig. 2) with s positive steps of equal magnitude E, it is well-known that the waveform's Fourier series expansion is given by

$$v_o(t) = \sum_{\text{odd } h} \{ V_h \sin(h\omega t) \} \quad (1)$$

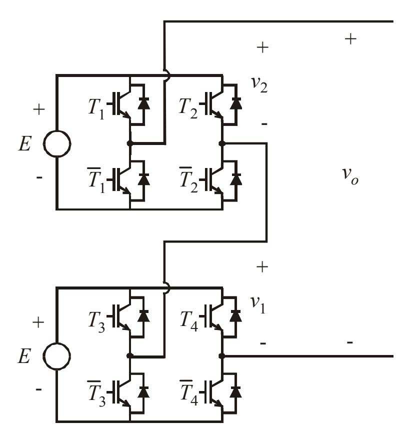

Figure 1. Cascaded H-bridge (2-cell) multilevel converter circuit

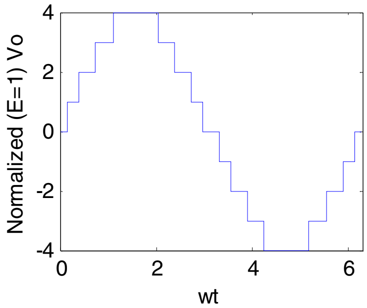

Figure 2. 4-step, 9-level waveform

where

$$V_h = \frac{4\,E}{h\,\pi}\,[\cos(h\theta_1) + \cos(h\theta_2) + \ldots + \cos(h\theta_s)] \qquad (2)$$

and the θ_i, $i = 1, \ldots, s$, are the angles (within the first quarter of each waveform cycle) at which the s steps occur. On the other hand, if a negative step (down) instead of a positive step (up) occurs at a particular θ_i, the coefficient of the corresponding cosine term in (2) is -1 instead of $+1$. Note that the even harmonics are all zero.

For the specific (introductory) problem of synthesizing a stepped waveform that has desired levels of V_1 and V_3 with two of the adjacent higher harmonics equal to zero, the stepping angles $0 \le \theta_1 < \theta_2 < \ldots < \theta_s \le \pi/2$ must be chosen so that

$$\frac{4\,E}{\pi}[\cos(\theta_1) + \cos(\theta_2) + \ldots + \cos(\theta_s)] = V_1 \qquad (3a)$$

$$\frac{4\,E}{3\,\pi}[\cos(3\theta_1) + \cos(3\theta_2) + \ldots + \cos(3\theta_s)] = V_3 \qquad (b)$$

$$\cos(5\theta_1) + \cos(5\theta_2) + \ldots + \cos(5\theta_s) = 0 \qquad (c)$$

$$\cos(7\theta_1) + \cos(7\theta_2) + \ldots + \cos(7\theta_s) = 0 \qquad (d)$$

Again, for a waveform with a step down instead of a step up occurring at a particular θ_i, the coefficient of the corresponding cosine term in (3) should be -1 instead of $+1$. Using the identities (also advocated by [8])

$$\cos(3\theta) = 4\cos(\theta)^3 - 3\cos(\theta) \qquad (4a)$$

$$\cos(5\theta) = 16\cos(\theta)^5 - 20\cos(\theta)^3 + 5\cos(\theta) \qquad (b)$$

$$\cos(7\theta) = 64\cos(\theta)^7 - 112\cos(\theta)^5 + 56\cos(\theta)^3 - 7\cos(\theta) \quad (c)$$

and defining c_i as $\cos(\theta_i)$, (3) can be re-written as

$$\sum_{i=1,..,s} c_i = V_1 / \frac{4\,E}{\pi} = m_1 \qquad (5a)$$

$$\sum_{i=1,..,s} \{\, 4\,c_i^3 - 3\,c_i \,\} = V_3 / \frac{4\,E}{3\,\pi} = m_3 \qquad (b)$$

$$\sum_{i=1,..,s} \{\, 16\,c_i^5 - 20\,c_i^3 + 5\,c_i \,\} = 0 \qquad (c)$$

$$\sum_{i=1,..,s} \{\, 64\,c_i^7 - 112\,c_i^5 + 56\,c_i^3 - 7\,c_i \,\} = 0 \qquad (d)$$

Thus the set of trigonometric equations (3) has been transformed into a set of multivariate polynomial equations (5), the solution of which is discussed in [9], for example. Clearly, a necessary condition for the existence of nontrivial solutions to (5) is that the number of steps s be greater than or equal to the number of constraint equations. Consider now the two most basic problems of dual- frequency output voltage approximation by multilevel inverters:

a. 2-step (s = 2) waveform with desired levels of 1st and 3rd harmonics, and

b. 3-step (s = 3) waveform with desired levels of 1st and 3rd harmonics and simultaneous elimination of the 5th.

A. 2-step waveform problem

There are two alternatives to consider: the PP case and PN case representing waveforms having two successive positive steps, and a positive step followed by a negative step, respectively (see Fig. 3). Their negations, the NN case and NP case, simply result in solutions that are 180° phase-shifted respectively from the PP and PN solutions.

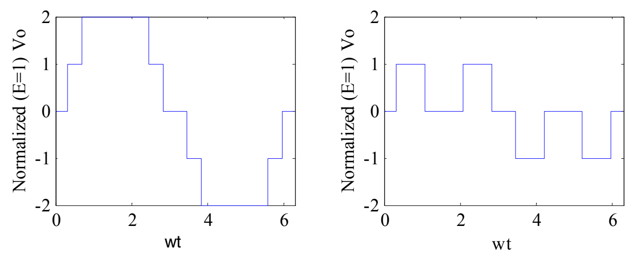

Figure 3. 2-step waveform alternatives (PP and PN)

(i) PP case

The applicable equations are, from (5a) and (5b),

$$c_1 + c_2 = m_1 \qquad (6a)$$

$$(4\,c_1^3 - 3\,c_1) + (4\,c_2^3 - 3\,c_2) = m_3 \qquad (b)$$

Solving for c_1 and c_2 yields

$$c_1 = [\,3m_1^2 + \sqrt{3(3m_1^2 - m_1^4 + m_1 m_3)}\,] / 6\,m_1 \qquad (7a)$$

$$c_2 = [\,3m_1^2 - \sqrt{3(3m_1^2 - m_1^4 + m_1 m_3)}\,] / 6\,m_1 \qquad (b)$$

From (6a), note that for admissible c_1 and c_2, m_1 is restricted to a value between 0 and 2. Moreover, since c_1 and c_2 need to be real and greater than 0, these constrain m_3 so that

$$m_1^3 - 3m_1 \le m_3 \le 4m_1^3 - 3m_1, \quad \text{for } 0 \le m_1 \le 1 \qquad (8a)$$

$$m_1^3 - 3m_1 \le m_3 \le 4m_1^3 - 12m_1^2 + 9m_1, \quad \text{for } 1 \le m_1 \le 2 \quad (b)$$

The plot of these constraint curves in Fig. 4 for m_3 versus m_1 indicates (and confirmed analytically) that the range of possible m_3 is maximized at $m_1 = 1$. Then for $m_1 = 1$, the solutions for θ_1 and θ_2 are (they are unique) as shown in Fig. 5 as m_3 varies and the corresponding frequency-weighted total harmonic distortion (THD) are as shown in Fig. 6. Note that $V_3/V_1 = m_3/(3m_1)$.

The solutions for θ_1 and θ_2 as well as the associated frequency-weighted THD were also obtained at other allowable values of m_1 and m_3, but these are not shown here due to space constraints. Note also that this case requires the production of a 5-level waveform and (at least) a 2-cell converter. With a 2-cell converter, it is possible to turn on and turn off each switch at the fundamental frequency to produce the desired waveform.

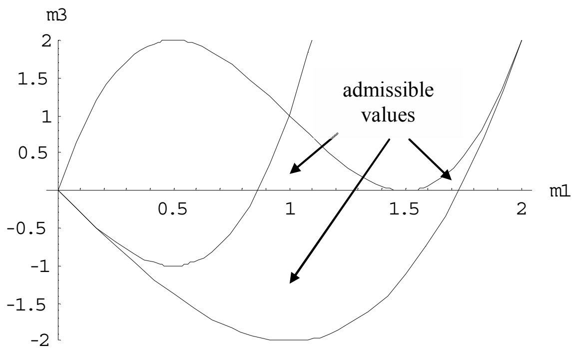

Figure 4. Constraint curves for m_3 versus m_1 (PP case)

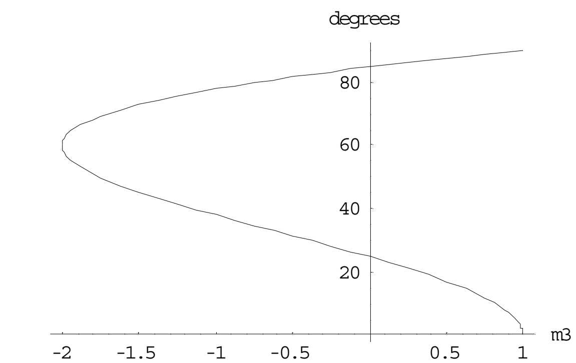

Figure 5. Step angle solutions for θ_1 (lower) and θ_2 (upper) when $m_1 = 1$

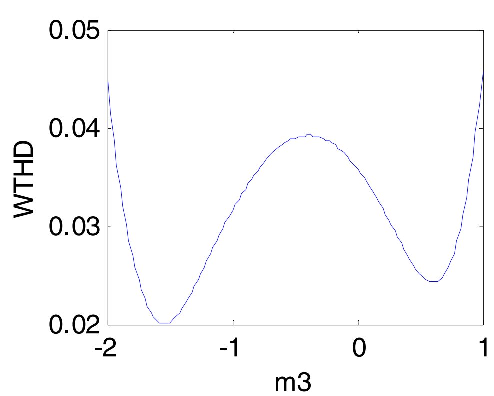

Figure 6. Frequency-weighted THD for $m_1 = 1$

(ii) PN case

The applicable equations are

$$c_1 - c_2 = m_1 \qquad (9a)$$

$$(4\,c_1^3 - 3\,c_1) - (4\,c_2^3 - 3\,c_2) = m_3 \qquad (b)$$

where the second equation is obtained instead of (6b) because the second step is down instead of up. Then substituting (9a) into (9b) and solving for c_1 and c_2 yields

$$c_1 = [\,3m_1^2 + \sqrt{3(3m_1^2 - m_1^4 + m_1 m_3)}\,]\,/\,6\,m_1 \qquad (10a)$$

$$c_2 = [\,-3m_1^2 + \sqrt{3(3m_1^2 - m_1^4 + m_1 m_3)}\,]\,/\,6\,m_1 \qquad (b)$$

From (9a), note that for admissible c_1 and c_2, m_1 is restricted to a value between 0 and 1. Moreover, since c_1 needs to be real and less than 1, this constrains m_3 such that

$$m_1^3 - 3m_1 \le m_3 \le 4m_1^3 - 12m_1^2 + 9m_1 \qquad (11a)$$

whereas since c_2 needs to be real and greater than 0, this constrains m_3 such that

$$m_1^3 - 3m_1 \le 4m_1^3 - 3m_1 \le m_3 \qquad (b)$$

The plot of the constraint curves in Fig. 7 for m_3 versus m_1 indicates (and confirmed analytically) that the range of possible m_3 yielding admissible solutions is maximized at $m_1 = 0.5$.

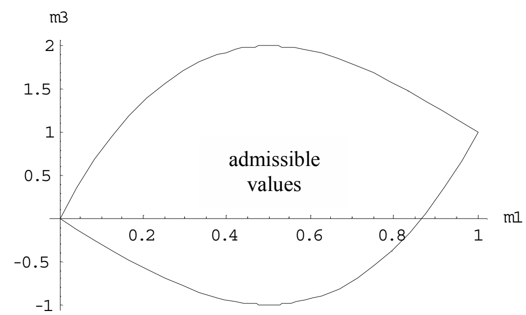

Figure 7. Constraint curves for m_3 versus m_1 (PN case)

Then for $m_1 = 0.5$, the step angle solutions for θ_1 and θ_2 (they are unique) as m_3 varies and the corresponding frequency-weighted THD are as shown in Fig. 8 and Fig. 9.

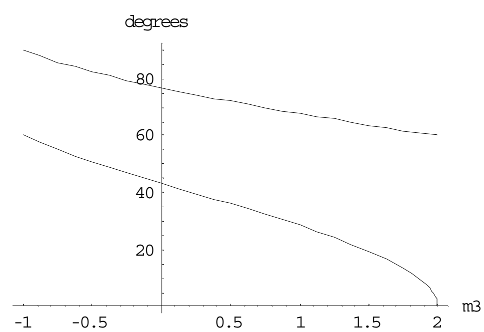

Figure 8. Step angle solutions for θ_1 (lower) and θ_2 (upper) for $m_1 = 0.5$

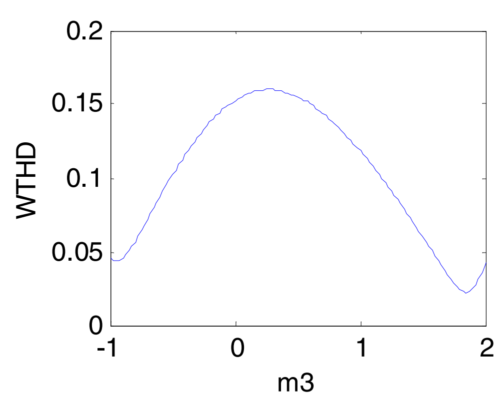

Figure 9. Frequency-weighted THD for $m_1 = 0.5$

The solutions for θ_1 and θ_2 as well as the associated frequency-weighted THD were also obtained at other allowable values of m_1 and m_3, but these are not shown here.

Note that this case requires the production of a 3-level waveform and (at least) a 1-cell converter. With a 1-cell converter, the switches can be operated so that each turns on and off at twice the fundamental frequency. With a 2-cell converter, it is possible to turn each switch on and off at the fundamental frequency to produce the desired waveform.

B. 3-step waveform problem

There are four, i.e., ½(2^3), possible combinations of 3-step waveforms to consider, excluding those that are the negations of the following cases: PPP, PPN, PNP and PNN.

The applicable equations are, from (5a), (5b) and (5c),

$$c_1 + k_2 c_2 + k_3 c_3 = m_1 \quad (12a)$$

$$(4 c_1^3 - 3 c_1) + k_2 (4 c_2^3 - 3 c_2) + k_3 (4 c_3^3 - 3 c_3) = m_3 \quad (b)$$

$$(16c_1^5 - 20c_1^3 + 5c_1) + k_2(16c_2^5 - 20c_2^3 + 5c_2) + k_3(16c_3^5 - 20c_3^3 + 5c_3) = 0 \quad (c)$$

where k_2, k_3 are separately either +1 or −1 for a positive step or a negative step, respectively. Substituting for c_3 from (12a) into (12b), (12c), then yields two (nonlinear) polynomial equations in terms of c_1 and c_2. The exact solution of such equations (as opposed to running a search algorithm) is, in general, computationally intensive and increasingly difficult as the number of variables increases [9]. For two equations with two variables, however, the procedure is relatively straight forward as summarized in the Appendix.

In each case, we first determined the limits of m_1 and m_3 for the existence of admissible solutions from (12). These limits are defined by the requirement for c_1, c_2, c_3 to be real and, by definition of their relationship, for c_1 to be less than 1 and c_3 to be greater than 0. Then, as example, the value of m_1 yielding the maximum range of m_3 was determined and the step-angles for this m_1 value found by solving (12) iteratively for incrementally increasing values of m_3. These solutions then allowed the higher harmonic amplitudes to be plotted.

(i) PPP case

Solutions exist and are probably unique (no multiple solutions have been found for the values of m_1 and m_3 tested so far) for the range of m_1 and m_3 delineated by the constraint curves of Fig. 10. The value of m_1 yielding the maximum range of m_3 is about 1.8. Plots of the step-angle solutions at this optimum and of the corresponding higher harmonic amplitudes are omitted due to length constraints. Note that this case requires the production of a 7-level waveform and (at least) a 3-cell converter. With a 3-cell converter, it is possible to turn on and turn off each switch at the fundamental frequency to produce the desired waveform.

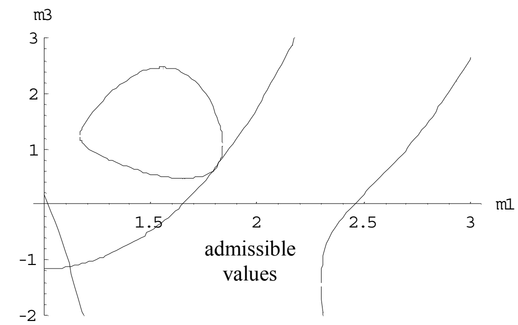

Figure 10. Constraint curves for m_3 versus m_1 (PPP case)

(ii) PPN case

Solutions exist and are probably unique (no multiple solutions have been found for the values of m_1 and m_3 tested so far) for the range of m_1 and m_3 delineated by the constraint curves of Fig. 11. The value of m_1 yielding the maximum range of m_3 is about 1.1. Plots of the step-angle solutions at this optimum and of the corresponding higher harmonic amplitudes are omitted due to length constraints. Note that this case requires the production of a 5-level waveform and (at least) a 2-cell converter. But with a 3-cell converter, it is possible to turn on and turn off each switch at the fundamental frequency to produce the desired waveform, which is not possible with a 2-cell converter.

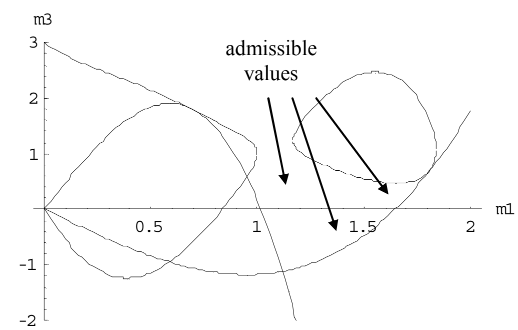

Figure 11. Constraint curves for m_3 versus m_1 (PPN case)

(iii) PNP case

Solutions exist and are probably unique (no multiple solutions have been found for the values of m_1 and m_3 tested so far) for the range of m_1 and m_3 delineated by the constraint curves of Fig. 12. The value of m_1 yielding the maximum range of m_3 is about 0.588. Plots of the step-angle solutions at this optimum and of the corresponding higher harmonic amplitudes are shown in Fig. 13 and Fig. 14, respectively. Note that this case requires the production of just a 3-level waveform and (at least) a 1-cell converter. But with a 3-cell converter, it is possible to turn on and turn off each switch at the fundamental frequency to produce the desired waveform, which is impossible with a 1- or 2-cell converter.

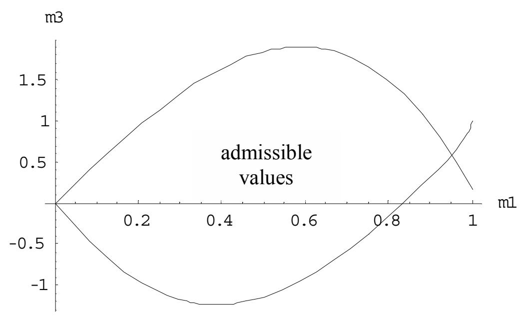

Figure 12. Constraint curves for m_3 versus m_1 (PNP case)

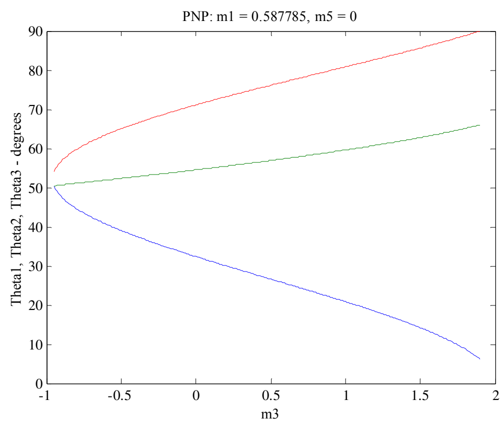

Figure 13. Step angle solutions for PNP case maximum m_3 range

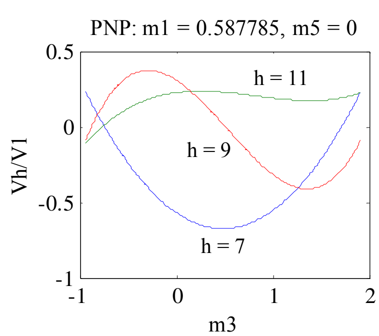

Figure 14. Ratios of V_7, V_9 and V_{11} to V_1

(iv) PNN case

Solutions exist and are probably unique (no multiple solutions have been found for the values of m_1 and m_3 tested so far) for the range of m_1 and m_3 delineated by the constraint curves of Fig. 15. The value of m_1 yielding the maximum range of m_3 is at 0, which is not useful. Plots of the step-angle solutions at this optimum and of the corresponding higher harmonic amplitudes are omitted due to the length constraint on this paper.

Note that this case requires the production of just a 3-level waveform and (at least) a 1-cell converter. But with a 3-cell converter, it is possible to turn on and turn off each switch at the fundamental frequency to produce the desired waveform, which is impossible with a 1- or 2-cell converter.

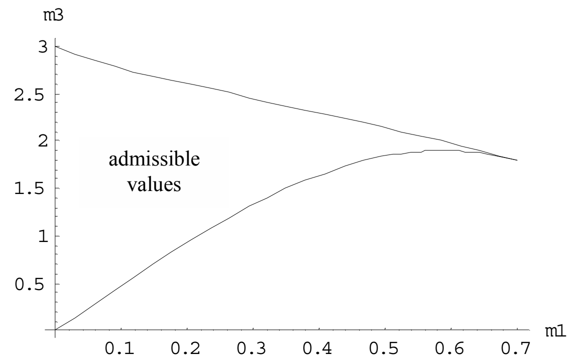

Figure 15. Constraint curves for m_3 versus m_1 (PNN case)

C. 4-*step waveform problem*

The above investigation was extended in a similar manner to the 4-step/4-equation problem (corresponding exactly to (3) with s = 4) with desired levels of 1st and 3rd harmonics and simultaneous elimination of the 5th and 7th harmonics, and then to the more practical problem of producing 1st and 5th harmonics with simultaneous elimination of the 3rd and 7th harmonics, which however cannot be detailed here due to space constraints.

III. Analysis – Unequal DC Source Values

Consider now the situation where the DC source values are not identical, which is more typical. For a quarter-wave symmetric waveform with s steps of magnitudes E_i, i = 1, … , s, its Fourier series expansion is given by (1) but with

$$V_h = \frac{4}{h\pi}[E_1\cos(h\theta_1) \pm E_2\cos(h\theta_2) \pm \ldots \pm E_s\cos(h\theta_s)] \quad (13)$$

where the θ_i, i = 1, … , s, are the angles (within the first quarter of each waveform cycle) at which the s steps occur and the signs are either + or – depending on whether a positive step or a negative step occurs at a particular θ_i.

For the specific (introductory) problem of synthesizing a stepped waveform that has desired levels of V_1 and V_3 with two of the adjacent higher harmonics equal to zero, the step angles $0 \le \theta_1 < \theta_2 < \ldots < \theta_s \le \pi/2$ must be chosen so that

$$\frac{4}{\pi}[\, E_1 \cos(\theta_1) \pm E_2 \cos(\theta_2) \pm \ldots \pm E_s \cos(\theta_s)] = V_1 \quad (14a)$$

$$\frac{4}{3\pi}[E_1 \cos(3\theta_1) \pm E_2 \cos(3\theta_2) \pm \ldots \pm E_s \cos(3\theta_s)] = V_3 \quad (b)$$

$$E_1 \cos(5\theta_1) \pm E_2 \cos(5\theta_2) \pm \ldots \pm E_s \cos(5\theta_s) = 0 \quad (c)$$

$$E_1 \cos(7\theta_1) \pm E_2 \cos(7\theta_2) \pm \ldots \pm E_s \cos(7\theta_s) = 0 \quad (d)$$

again with the signs being either + or – depending on the corresponding step direction. Next, applying the identities in (4) and defining $\rho_i = E_i / E_s$, allow (14) to be re-written as

$$\sum_{i=1,\ldots,s} \rho_i\, c_i = V_1 / \frac{4\,E_s}{\pi} = m_1 \quad (15a)$$

$$\sum_{i=1,\ldots,s} \rho_i \,\{\, 4\, c_i^3 - 3\, c_i \,\} = V_3 / \frac{4\,E_s}{3\,\pi} = m_3 \quad (b)$$

$$\sum_{i=1,\ldots,s} \rho_i \,\{\, 16\, c_i^5 - 20\, c_i^3 + 5\, c_i \,\} = 0 \quad (c)$$

$$\sum_{i=1,\ldots,s} \rho_i \,\{\, 64\, c_i^7 - 112\, c_i^5 + 56\, c_i^3 - 7\, c_i \,\} = 0 \quad (d)$$

This set of multivariate polynomial equations can then be solved using the same procedures as for the case of equal source values. Unfortunately, in general, there is apparently not a simple relationship between these solutions and those solutions for the equal source case that can be exploited. Considering the PNP case as example, with E_1 = 0.9, E_2 = 1.1, E_3 = 1, the step-angle solutions obtained for m_1 = 0.587785 and varying m_3 are shown in Fig. 16: note the difference from the equal source solutions shown in Fig. 13. Clearly, other source values and/or the other step-pattern cases can be treated accordingly.

IV. Experimental Results

Laboratory measurements were obtained from a 5-level inverter demonstrating the unequal DC source (with $E_1 = E_2 = E_3$ = 200V, E_4 = 67V) 4-step PNPP case as example, to generate desired 1st and 5th harmonic levels with V_5/V_1 = 1.0 while canceling the 3rd and 7th harmonics. This waveform may be desired for an application where a span of 5 is needed between the two heating frequencies. The step angles were set to θ_1 = 9.09°, θ_2 = 34.43°, θ_3 = 69.73°, θ_4 = 74.17° (as appropriately calculated). Fig. 17 shows the voltage and current waveforms for a fundamental frequency of 10kHz. The *R-L* load average power was 437.5W and conversion efficiency was estimated to be 95.6% (from estimate of the IGBT dual-module losses based on datasheet values). Table 1 shows a comparison of the analytical and measured voltage harmonic amplitudes indicating good agreement between them. Note that the higher harmonics are mostly filtered out by the load inductance resulting mainly in the desired dual-frequency current as shown in Fig. 18.

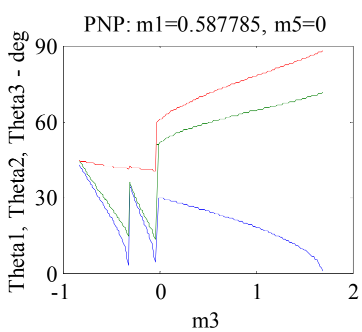

Figure 16. Step angle solutions for PNP case with unequal sources

Table 1. Unequal source 4-step 5-level inverter voltage harmonics.

	V_1	V_3	V_5	V_7	V_9	V_{11}	V_{13}	V_{15}
Analytical	153.0	0	153.0	0	10.0	12.0	32.5	22.9
Measured	145.3	8.4	150.0	6.1	1.7	9.7	33.2	22.8

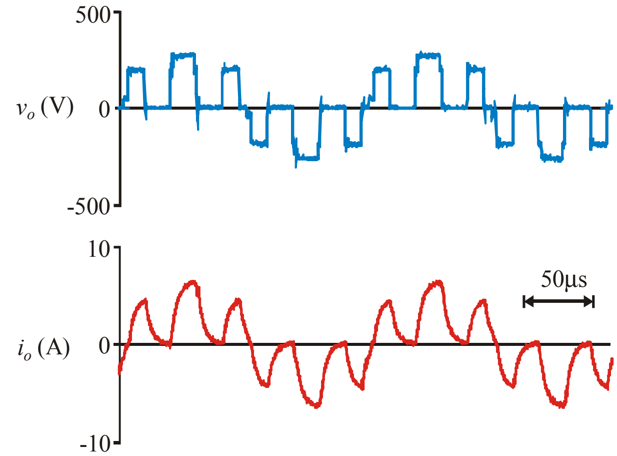

Figure 17. Unequal source 4-step, 5-level inverter waveforms.

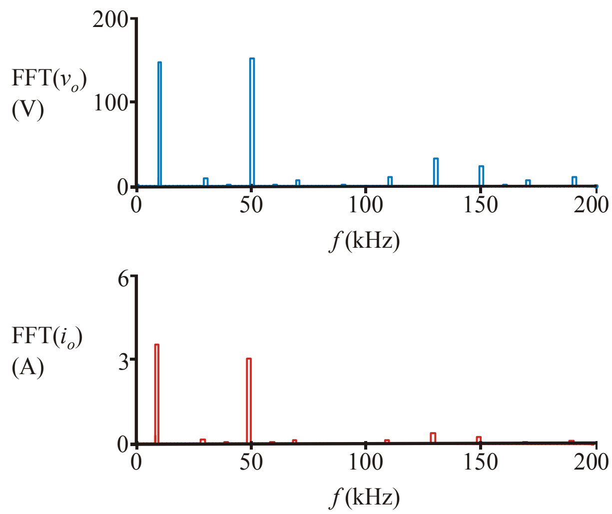

Figure 18. Unequal source 4-step, 5-level inverter output spectrums.

V. Conclusions

Fundamental results have been presented on the use of multilevel inverters for producing power at two frequencies simultaneously, as desirable for certain induction heating applications. A complete analysis has been shown for the 2-step case and for the 3-step case, considering either equal or unequal DC sources.

For the 2-step case (with equal sources) to generate desired levels of 1st and 3rd harmonics, the PP waveform results in lower harmonic distortion compared to the PN waveform but requires a 5-level waveform instead of a 3-level waveform. Moreover, for required magnitudes of $m_3 \leq 1$ with the PP waveform, positive m_3 is preferable to negative m_3 for reduced distortion. However, the PN waveform allows a broader range of achievable 1st and 3rd harmonic level combinations.

For the 3-step case (with equal sources), the PNP waveform allows for a broad range of achievable 1st and 3rd harmonic level combinations although yielding a fair amount of harmonic distortion. Moreover, it only requires producing a 3-level waveform. However, to have all devices operate at the fundamental frequency to produce this waveform still requires a 3-cell converter.

Finally, experimental results have been presented for the unequal source 4-step case that validates the proposed approach to dual-frequency voltage generation by multilevel inverters with equal or unequal DC sources. Unfortunately, the analysis also suggests there is no simple relationship between the solutions for the unequal source case and those solutions for the equal source case.

REFERENCES

[1] K. Matsuse, K. Nomura and S. Okudaira, "New quasi-resonant inverter for induction heating," *Power Conversion Conference, 1993. Yokohama 1993. Conference Record of the*, pp. 117–122.

[2] K. Matsuse and S. Okudaira, "Power control of an adjustable frequency quasi-resonant inverter for dual frequency induction heating," *Proc. PIEMC*, 2000, vol. 2, pp. 968–973.

[3] S. Okudaira and K. Matsuse, "Dual frequency output quasi-resonant inverter for induction heating," *Trans. Institute of Electrical Engineers of Japan*, vol. 121-D, no. 5, pp. 563–568, May 2001.

[4] K. Matsuse and S. Okudaira, "A new quasi-resonant inverter with two-way short-circuit switch across a resonant capacitor," *Proc. Power Conversion Conf., Osaka*, 2002, vol. 3, pp. 1496–1501.

[5] http://www.eldec.de/engl/download/SDF-method.pdf; *Simultaneous Dual Frequency Induction Heat Treating.*

[6] J. Rodriguez, J-S. Lai and F. Z. Peng, "Multilevel inverters: a survey of topologies, controls, and applications," *IEEE Trans. Industrial Electronics*," vol. 49, pp. 724–738, Aug 2002.

[7] J. I. Rodriguez and S. B. Leeb, "A multilevel inverter topology for inductively-coupled power transfer," *Applied Power Electronics Conf.*, 2003, Eighteenth Annual IEEE, vol. 2, pp. 1118–1126.

[8] J. Chiasson, L. Tolbert, K. McKenzie and Z. Du, "Eliminating harmonics in a multilevel converter using resultant theory," *Power Electronics Specialists Conf.*, 2002, vol. 2, pp. 503–508.

[9] D. Cox, J. Little and D. O'Shea, *Using algebraic geometry*, Springer, New York, 1998.

APPENDIX

Fact [9]: Given two polynomials

$$f(x, y) = a_0(x)\, y^l + a_1(x)\, y^{l-1} + \ldots + a_l, \quad a_0(x) \neq 0, \quad l > 0$$

$$g(x, y) = b_0(x)\, y^n + b_1(x)\, y^{n-1} + \ldots + b_n, \quad b_0(x) \neq 0, \quad n > 0$$

all possible solutions (x^*, y^*) of $f(x, y) = 0$ and $g(x, y) = 0$ can be obtained by finding x^* as the eigenvalues of the Sylvester matrix formed from the $a_j(x)$, $j = 1, \ldots, l$, and $b_k(x)$, $k = 1, \ldots, n$, and then y^* as the roots of $f(x^*, y) = 0$.

Procedure for calculating the 3-step angle solutions:

1. From (12a), substitute $c_3(c_1, c_2)$ into (12b) and (12c) to obtain two polynomial equations in c_1 and c_2.
2. From the two polynomials $f(c_1, c_2)$ and $g(c_1, c_2)$, extract the coefficients of the powers of c_2 and label them appropriately as $a_0, a_1, \ldots, a_l, b_0, b_1, \ldots, b_n$.
3. Form the Sylvester matrix [9] from these coefficients and then find its eigenvalues. These eigenvalues are the candidate solutions for c_1 in our problem, which also needs to be a real number and satisfy $0 \leq c_1 \leq 1$; so discard the inadmissible ones.
4. For each remaining candidate solution for c_1, substitute its value into $f(c_1, c_2)$ and find the candidate solutions for c_2 in our problem, which needs to be a real number and satisfy $0 \leq c_2 \leq c_1$; so discard the inadmissible ones.
5. For each remaining candidate solution for c_2, substitute its value and the corresponding candidate solution for c_1 into (12a) to find the candidate solution for c_3, which needs to be a real number and satisfy $0 \leq c_3 \leq c_2$ to be admissible.
6. The admissible triples of (c_1, c_2, c_3) are then the solution(s) to the 3-step waveform problem.